HEAT LOAD DISTRIBUTION IN CASE OF SUDDEN BEAM LOSS FOR ALBA-II

O. Blanco-García*, U. Iriso†, ALBA Synchrotron (Spain), Cerdanyola del Vallès, Spain

Abstract

The upgrade of ALBA into a fourth generation of synchrotron light source, ALBA II, foresees to reduce the electron beam emittance to about 200 pm while increasing the beam current to 300 mA. This combination increases the risk of damage to elements in the accelerator when the beam is lost in a controlled or uncontrolled manner. We simulate the electron beam particle loss distribution for the most recent design of the ALBA-II lattice with errors and corrections, and use these results to estimate the heat load to which the vacuum chamber would be exposed. Initial considerations on beam scrapers and abort systems are presented.

INTRODUCTION

ALBA is a third generation, 3 GeV synchrotron light source with a natural emittance of 4.6 nm [1, 2]. At ALBA, and in most of the 3rd generation of synchrotron light sources, in case of a sudden beam loss the interlock system generally sends a signal to switch off the RF system. The beam then starts to lose energy and in ~hundreds of turns, the beam hits the vacuum chamber all around the accelerator and is lost. Over the 15 years of operation at ALBA none of the electron beam losses have damaged the beam pipe or nearby objects.

ALBA is currently going to an upgrade called ALBA-II [3, 4], where the beam energy is kept at 3 GeV, but the emittance is reduced to 200 pm. The machine upgrade has to comply with several constraints imposed by the decision of maintaining the same circumference (269 m), the same number of cells (16), and keep as many of the source points as possible unperturbed.

Several machines have already gone through a similar path, from 3rd to 4th generation of synchrotron light sources. In some cases, their studies have shown that switching off the RF system produces a beam loss pattern with very high losses in specific locations of the ring producing fatal damages, like vacuum leaks in the vacuum chamber or demagnetization of the permanent magnets. Few of them have designed specific beam dump systems: this is the case for example for APS-U [5], SLS 2.0 [6], or Diamond-II [7]. For these reasons, we have also studied the beam dump process for ALBA-II.

ALBA-II AND BEAM LOSS MODELING

The single particle energy loss per turn in ALBA-II is expected to be close to 900 KeV from bendings in the lattice design and about 150 KeV from the photon radiation on the straights with insertion devices. It amounts to 0.04% of the nominal beam energy which is smaller that the beam energy spread of 0.1%.

This energy loss is balanced by an RF system distributed over two sectors of the ring, which includes 6 main RF cavities, plus 4 additional harmonic cavities to enlarge the bunch length and increase the Touscheck lifetime [8, 9].

There are several scenarios for the sudden loss when the RF cavities are turned off. The most severe is the sudden and complete loss of power on the RF cavities, which occurs in 4 µs, or equivalently 4 to 5 beam turns around the ring. Over this period, the voltage seen by the beam drops from the nominal 2.4 MV to zero. Next the interaction of the beam and RF system induces a voltage on the RF cavities that further decelerates the beam, see Fig. 1. The cumulative energy loss reduces the number of turns before the beam collides with the beam pipe in different locations to about 60 with respect to 80 turns if the cavities were not there.

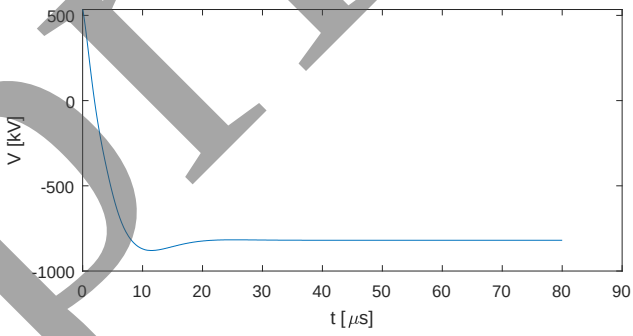

Figure 1: RF voltage vs time in one of the modules composing the RF system seen by a synchronous particle when the RF is switched off. The final voltage is induced by beam loading of the full stored beam, assuming no losses.

Physical apertures are modeled in detail. The initial round vacuum chamber of 16 mm inner diameter [3], has been replaced by an alternative rhombic chamber with transverse inner dimensions 20 mm wide and 14.8 mm high to increase the horizontal distance between any obstacle and the injected beam [10]. The simulations here presented consider the latter, except explicit mention of the former. Apart from the generic beam pipe dimensions, the insertion devices gaps, septum position, and scrapers are included.

The storage ring design for ALBA-II is subject to performance studies where errors and corrections are put together in order to estimate the likelihood of injection efficiency and Touschek lifetime [11]. Those ring models coming out of simulations have been used to perform the calculation of beam loss distribution.

A set of 100 rings with errors and corrections are used for particle tracking. Each ring is an individual simulation where an electron beam represented as 4 bunches with 4000 particles each is tracked from 1 turn before the RF is turned

* oblanco@cells.es
† ubaldo.iriso@cells.es

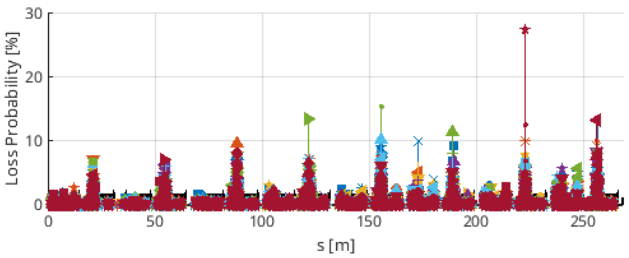

Figure 2: Particle beam loss distribution along the ring. Different colors and markers indicate the result of different simulations

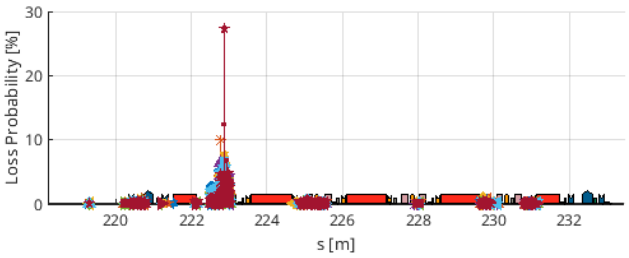

Figure 3: Particle losses in one sector.

off to the end of all particles in tracking, using Accelerator Toolbox (AT) [12]. The AT RF cavities model have been replaced by a custom voltage profile based on the RF system data, as in Fig.1, that takes in account the particle time of arrival and bunch population. The element and turn where the particles are lost are recorded including the particle 6D phase space position at the entry point of the last element they cross.

Figure 2 shows the distribution of the particle losses along the ALBA-II storage ring. In general, independently of the errors and corrections we deal with, it is expected that electron beam losses will be distributed all along the ring with a very small fraction of few % at a particular location. When zooming in an individual sector, there is a common pattern where the particle losses appear to concentrate after the first dipole, see Fig. 3. The combination of dispersion and horizontal beta function makes the particles get closer to the acceptance boundary than in any other point. The x-δ acceptance of the ring is shown in Fig. 4 using Flood Fill [13]. We remark that detailed physical apertures have been modeled but have negligible impact on the acceptance. Particles initially stable on the ring slowly lower their energy on every turn until they reach the bottom of the acceptance before the physical aperture, therefore, their motion becomes chaotic and spreads the particles around the ring.

There are still rare but possible cases where the beam loss exceeds the 10% at a particular element and for a particular ring. We have gone into further details trying to analyze the characteristics of these losses. We discarded the effect of a wrong correction of the ring; it is in fact a ring with a valid closed orbit, linear optics beta-beat, dynamic aperture for injection and Touschek lifetime similar to others.

The highest loss happens over a drift of 7 cm which we call "D7CM". We have taken the particle distribution at the

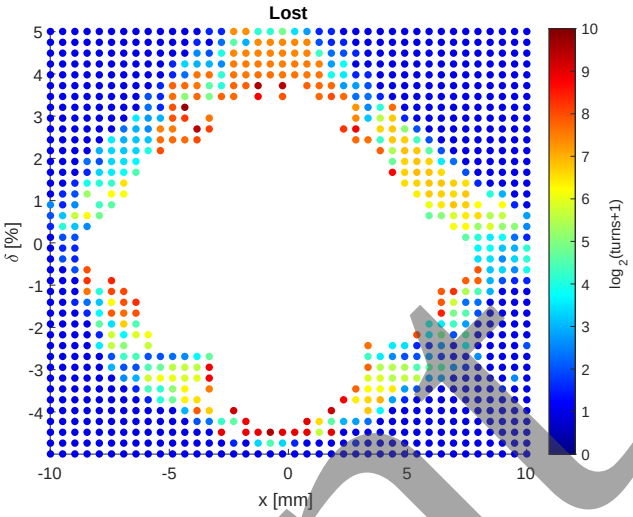

Figure 4: $x - \delta$ acceptance of the ring without physical aperture seen at the injection section. Color scale represents the number of turns the particle survived.

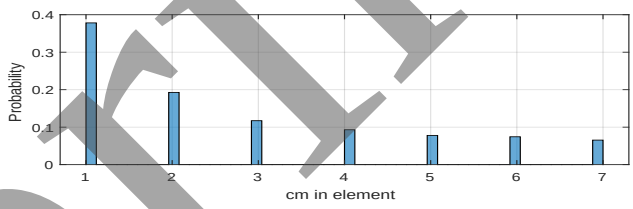

Figure 5: Normalized particle losses inside the 7 cm drift.

beginning of the drift and tracked over that single element sliced in pieces of 1 cm each. This allows us to determine with more precision the exit point of those particles. The particle distribution on the phase space shows several points to take into account:

- Losses occur mostly on the horizontal plane.
- The transverse beam size just before the loss is around (200, 35) µm. In case of perpendicular impact it implies a large particle density.
- The recent change to a rhombic vacuum chamber increases the distance between the beam motion and the photon radiation absorbers making the losses less likely to concentrate there.
- Particles enter with a horizontal angle ranging from 1 to 10 mrad, typically 5 mrad, which means that particles hit the beam pipe in a shallow angle, spreading the dense 200 µm in the horizontal plane to several cm from the angle projection into the vacuum pipe wall.

Figure 5 shows the particle tracking results over the 7 cm long drift. The minimum vertical beam size is 35 µm and the particle losses appear distributed all along with a maximum at the entry point.

EFFECT OF SCRAPERS

In general, it would be preferred to absorb part of the losses in regions where damage is limited and controlled.

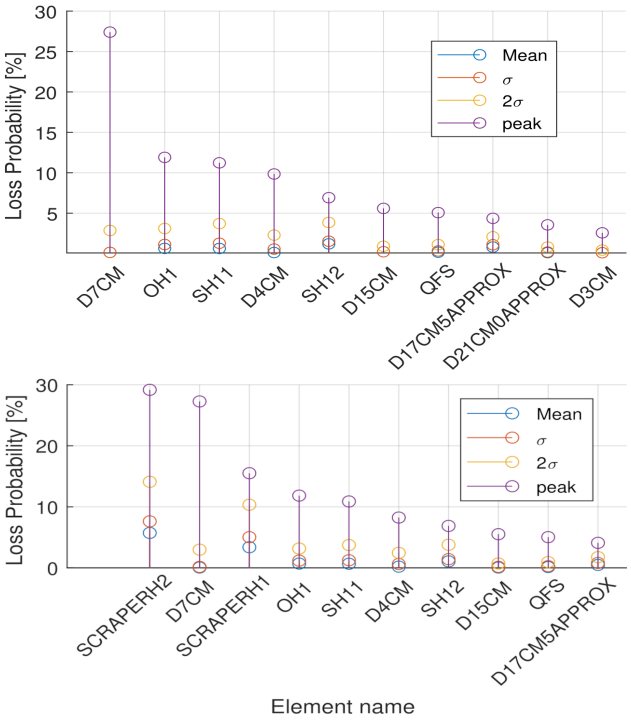

Figure 6: Effect of scrapers in the ALBA II storage ring. (TOP) Ten elements with highest loss ranking without scrapers. (BOTTOM) Same ranking with scrapers at -6 mm from beam center. The plot shows the statistics from 100 rings: the mean, the σ (68%) and 2σ (95%) and the peak loss.

For this reason, we study the effect of installing horizontal scrapers with a water cooling system. In a balance between effectiveness and space availability, we study the possibility of installing two horizontal scrapers in Sectors 1 and 9 of the ring, just after the first bending of the arc where the dispersion rises.

Figure 6 compares the effect of the loss distribution in a ring without scraper (top) and with scrapers (bottom). With scrapers, up to 30% of losses due to absence of RF power is absorbed, and they also reduce the mean losses all over the ring. Still there are certain lattices where the scrapers are ineffective, and for which additional considerations are being studied. Following the model in [7], we consider a vertical deflector that triggers upon the beam loss signal to increase the vertical emittance and decrease the beam energy density.

HEAT LOAD ESTIMATIONS

We calculate the temperature rise in the vacuum chamber at the machine location with highest losses. As shown in Fig. 6, in absence of the horizontal scraper this corresponds to the so-called "D7CM".

Analytical expressions have been derived in [14, 15] in order to estimate the temperature increase from the interaction of particles and matter. When a beam of N_e electrons hits a solid target whose thickness is smaller than the material radiation length, the temperature increase is [14]

$$\Delta T = S_{pc} \frac{A_w}{C_m} \frac{N_e}{2\pi\sigma_x\sigma_y} , \qquad (1)$$

where D is the dose in Gy or J/kg, A_w is the atomic weight in Kg/mole and C_m is the molar specific heat in J/kg/mole. (σ_x, σ_y) are the transverse dimensions of the beam hitting the chamber. The parameter $S_{\rm pc}$ is the collisional stopping power, which corresponds to the energy loss into ionization, and directly results in heating of the material. This value can be found in the NIST database [16]. Taking into account the footprint from the tracking simulations in Fig. 5, we assume a beam distribution of 35 µm in the vertical plane, and 1 cm in the longitudinal direction (which becomes horizontal when it crosses the vacuum chamber). Furthermore, we consider the worst case in which 27% of the 300 mA beam is lost at that location, from which a peak of 35% in the first 1-cm. Since the vacuum chamber material is Copper, using Eq. (1), we obtain $\Delta T = +5$ K of temperature increase.

This value of temperature increase is small, and gives the order of magnitude we could expect from real losses. Nevertheless, we plan to perform more detailed simulations using FLUKA [17] to precisely evaluate the heat load deposition and its consequences in the vacuum chamber.

SUMMARY

ALBA II beam losses when the RF system is turned off were studied in detail. The energy loss in bending magnets, insertion devices and beam loading in RF cavities has been modelled for the most recent design of the storage ring. Physical apertures are included but do not impact the $x - \delta$ acceptance leading to losses spread along the ring when the motion becomes chaotic. Statistical results have been simulated for 100 lattices with errors and corrections. In rare cases the beam loss exceeds the 10% in a single element. Most of the losses occur in the upstream part of the sector.

The peak losses have been tracked in detail in order to determine the characteristics of the beam impinging the beam pipe. A theoretical estimation of the temperature change of the vacuum pipe wall has been done showing an increase of less than 10 K due to the shallow angle between the beam and the wall at impact.

All the above indicates that sudden losses in ALBA-II do not represent a threat to the integrity of the vacuum chamber and therefore the accelerator operation. Nevertheless, it is preferable to have a manner to absorb part of the beam loss in a localized manner, and thus installation of scrapers has been studied. Furthermore, we do not discard the need for other mechanisms to decrease the beam density upon impact.

ACKNOWLEDGMENTS

The authors would like to thank M. Aiba from SLS for fruitful discussions on the topic of controlled beam loss, the ALBA RF group for explanations and information on the system performance, and A. Devienne from CERN for his support in the FLUKA simulations.

REFERENCES

[1] D. Einfeld et al, in *Proc. IPAC'11*, San Sebastian, Spain, Sep. 2011, paper MOXAA01, pp. 1–5. https://proceedings.jacow.org/IPAC2011/papers/moxaa01.pdf

[2] F. Perez, "First Year Operation of the ALBA Synchrotron Light Source", in *Proc. IPAC'13*, Shanghai, China, May 2013, paper MOPEA055, pp. 202–204.

[3] F. Perez *et al.*, "ALBA II accelerator upgrade project status", in *Proc. IPAC'24*, Nashville, TN, USA, May 2024, pp. 1220–1223. doi:10.18429/JACoW-IPAC2024-TUPG02

[4] F. Pérez et al, "ALBA II Accelerator Upgrade Project Status", presented at the IPAC'26, Deauville, France, May 2026, paper THP2009, this conference.

[5] M. Borland *et al.*, "Using Decoherence to Prevent Damage to the Swap-Out Dump for the APS Upgrade", in *Proc. IPAC'18*, Vancouver, Canada, Apr.-May 2018, pp. 1494–1497. doi:10.18429/JACoW-IPAC2018-TUPMK004

[6] F. Armborst *et al.*, "Commissioning of the SLS 2.0 machine protection system", in *Proc. IPAC'25*, Taipei, Taiwan, Jun. 2025, pp. 1278–1281. doi:10.18429/JACoW-IPAC2025-TUPM057

[7] H. Ghasem *et al.*, "Collimator damage study for the Diamond-II storage ring", in *Proc. IPAC'25*, Taipei, Taiwan, Jun. 2025, pp. 462-465. doi:10.18429/JACoW-IPAC2025-MOPM063

[8] F. Perez *et al.*, "ALBA II accelerator upgrade project status", in *Proc. IPAC'25*, Taipei, Taiwan, Jun. 2025, pp. 706–709. doi:10.18429/JACoW-IPAC2025-MOPS043

[9] I. Bellafont, F. Perez, and P. Solans, "Longitudinal beam dynamics studies with a third harmonic RF system for ALBA-II", in *Proc. IPAC'23*, Venice, Italy, May 2023, pp. 3534–3537. doi:10.18429/JACoW-IPAC2023-WEPL179

[10] R. Parise, *et al.*, "ALBAII Vacuum System: Design Evolution and Prototyping", presented at the IPAC'26, Deauville, France, May 2026, paper MOP7096, this conference.

[11] G. Benedetti, O. Blanco-García, M. Carlà, Z. Martí, and F. Perez, "Status of lattice studies for ALBA-II", presented at the IPAC'26, Deauville, France, May 2026, paper WEP5034, this conference.

[12] A.T. Collaboration, "Accelerator Toolobox", https://github.com/atcollab/at

[13] E. Serra-Carbonell, O. Blanco-García, and T. Günzel, "Application of fast algorithms to calculate dynamic and momentum aperture to the design of ALBA II", in *Proc. IPAC'25*, Taipei, Taiwan, Jun. 2025, pp. 197–200. doi:10.18429/JACoW-IPAC2025-MOPB065

[14] J. Dooling *et al.*, "Using Decoherence to Prevent Damage to the Swap-Out Dump for the APS Upgrade", in *Proc. IPAC'18*, Vancouver, Canada, Apr.-May 2018, pp. 1494–1497. doi:10.18429/JACoW-IPAC2018-TUPMK004

[15] J. Dooling *et al.*, "Collimator irradiation studies in the Argonne Advanced Photon Source at energy densities expected in next-generation storage ring light sources", *Phys. Rev. Accel. Beams*, vol. 25, no. 4, Apr. 2022. doi:10.1103/physrevaccelbeams.25.043001

[16] https://physics.nist.gov/PhysRefData/Star/Text/ESTAR.html

[17] https://fluka.cern